

# LEUKOCYTE RELAXATION PROPERTIES

KUO-LI PAUL SUNG,\* CHENG DONG,<sup>†</sup> GEERT W. SCHMID-SCHÖNBEIN,<sup>‡</sup> SHU CHIEN,\* AND RICHARD SKALAK<sup>§</sup>

\**Department of Physiology, College of Physicians and Surgeons, Columbia University, New York, NY 10032;* <sup>†</sup>*Bioengineering Institute, Dept. of Civil Engineering and Engineering Mech., Columbia University, New York, NY 10027;* and <sup>‡</sup>*Applied Mechanics and Engineering Sciences Bioengineering, University of California, San Diego, La Jolla, California 92093*

**ABSTRACT** Study of the mechanical properties of leukocytes is useful to understand their passage through narrow capillaries and interaction with other cells. Leukocytes are known to be viscoelastic and their properties have been established by micropipette aspiration techniques. Here, the recovery of leukocytes to their normal spherical form is studied after prolonged deformation in a pipette which is large enough to permit complete entry of the leukocyte. The recovery history is characterized by the time history of the major diameter ( $d_1$ ) and minor diameter ( $d_2$ ). When the cell is removed from the pipette, it shows initially a small rapid recoil followed by a slower asymptotic recovery to the spherical shape. In the presence of cell activation and formation of pseudopods, the time history for recovery is prolonged compared with passive cell recovery. If a protopod pre-existed during the holding period, the recovery only begins when the protopod starts to retract.

## INTRODUCTION

Knowledge of the rheological properties of individual leukocyte is useful for detailed understanding of their dynamic behavior in transport through narrow vessels and during migration out of the blood vessels. Usually, neutrophils and macrophages utilize lytic enzymes (Nathan et al., 1982) and lymphocytes utilize cytolytic killing or antibodies to mediate against or repel disease (Martz, 1975).

The white blood cells are significantly more resistant to deformation than the red blood cells and individual white blood cell can obstruct capillary blood flow, the so-called leukocyte plugging phenomenon (Nicoll and Webb, 1946; Schmid-Schönbein, 1987). Leukocyte plugging may occur whenever the diameter of a vessel is appreciably less than that of a white blood cell, the main reason for leukocyte plugging being the rigid character of individual white blood cell and the adhesion to the endothelium. The high resistance to deformation by leukocytes is also seen in micropipette studies in vitro which show that the pressure required to deform white blood cells is much higher than that required to deform red blood cells (Chien et al., 1980). Therefore, white blood cells impose a much larger resistance in capillary blood vessels than red blood cells (Bagge et al., 1977). In hypotensive states this may lead to plugging of white blood cells at the entrance to capillary vessels and thus cessation of flow (Bagge et al., 1980). In such large deformations involving the whole cell, the rheological behavior is determined by the geometry of the cell and the behavior of the nucleus, as well as the properties of the cytoplasm. After a leukocyte enters into a

capillary its resistance is dependent on the rate of relaxation back to the undeformed state. The present study is carried out to investigate the properties of individual cells during recovery after aspiration into a large pipette and subsequent release into suspension.

## EXPERIMENTAL METHODS

### Cell Material and Micropipette Set-Up

Human peripheral blood samples (10–20 ml) were obtained from the medial or lateral antecubital vein of several laboratory personnel volunteers (age 28–36 yr) with EDTA as the anticoagulant. The erythrocytes were allowed to sediment at room temperature for ~45 min. The supernatant plasma with leukocytes and platelets was collected with a Pasteur pipette and suspended in a saline solution with 12 mM Tris and bovine serum albumin (0.25 g/100 ml) at pH = 7.4 (by dropwise addition of HCl). The osmolarity was 310 mOsm. The buffer solution was filtered through a 0.2  $\mu$ m sterile Nalgene filter unit (Nalge Co., Div. of Sybron Corp., Rochester, NY) before usage. The final leukocyte count was ~40 cells/mm<sup>3</sup>. The prepared leukocytes were studied between 3/4 to 4 h after phlebotomy. The studies were performed at room temperature (21–23°C). The experimental setup was the same as used for our previous leukocyte experiments (Sung et al., 1982). About 1 ml of cell suspension was loaded in a small chamber with transparent bottom on an inverted microscope with 100 $\times$  objective (numerical aperture of 1.25, oil immersion) and 20 $\times$  eyepieces. The microscope was connected to a closed circuit TV system. Neutrophilic leukocytes were identified by their relatively small and numerous granules and viewed on a TV monitor at a final magnification of ~8,000. Length was calibrated with a 50  $\times$  2  $\mu$ m stage micrometer; Graticules LTD, Towbridge Kent, England). The video image was recorded on a video tape recorder together with time from a video time (IPM, San Diego, CA).

Micropipettes were pulled using a micropipette puller (Narshige Scientific Laboratory, Tokyo, Japan) to an internal radius 5–7  $\mu$ m for aspiration of the cells and to ~2  $\mu$ m for a separate set of holding pipettes. This dual micropipette system is similar to previous lymphocyte experi-

ments (Sung et al., 1986). The micropipettes were filled with buffer solutions and mounted on two hydraulic micromanipulators to the right and left of the microscope stage. The wide end of the micropipettes was connected to a pressure regulating and recording system which allowed step pressures and steady pressures to be imposed.

Measurements of cell dimensions were made during replay of the video tape by means of an image splitting device (IPM, San Diego, CA) and also with a digital image analysis system (Eye Company, Melbourne, FL).

## Experimental Protocol

Individual cells were aspirated into the larger pipette until they completely entered (Fig. 1, *a* and *b*). This process required typically 8–20 s and there was no apparent injury to the cell, such as swelling. Thereafter the cell was kept in the compressed state for a holding period, and was gently moved in a straight segment of the pipette to prevent glass adhesion. The majority of the cells showed no protopod projection during the holding period. After the holding period, the cell was gently pushed out of the pipette into the free medium to allow relaxation under uniform hydrostatic pressure. Cell movement was prevented by holding it gently with a smaller pipette. In this way a precise recovery record from a sharply focused cell could be obtained (Fig. 1, *a–i*).

Since cells without protopods are axisymmetrically deformed in this situation, the initial shape of the cell was defined by the major and minor diameters,  $d_1$  and  $d_2$  respectively, which were measured during the entire recovery period.

## MATHEMATICAL MODELING AND THEORY

In the following we assume the individual leukocytes are entirely aspirated into a large micropipette and held in a sausage shape for a long time before their recovery. Similar to the reference by Schmid-Schönbein et al. (1981), the leukocyte is considered as an incompressible standard viscoelastic solid body (Fig. 2 *a*) and axisymmetrically deformed (Fig. 2 *b*) without active protopod formation.

Let  $\sigma_{ij}$  be the stress components inside the leukocyte (see Fung, 1965, for notation conventions). The stress deviator  $v_{ij}$  is then defined in the cartesian coordinate system as ( $i, j = 1, 2, 3$ )

$$\tau_{ij} = \sigma_{ij} + p\delta_{ij}, \quad (1)$$

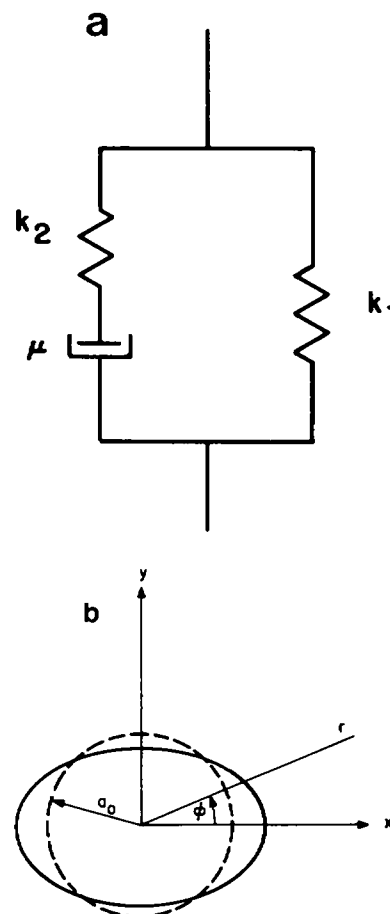
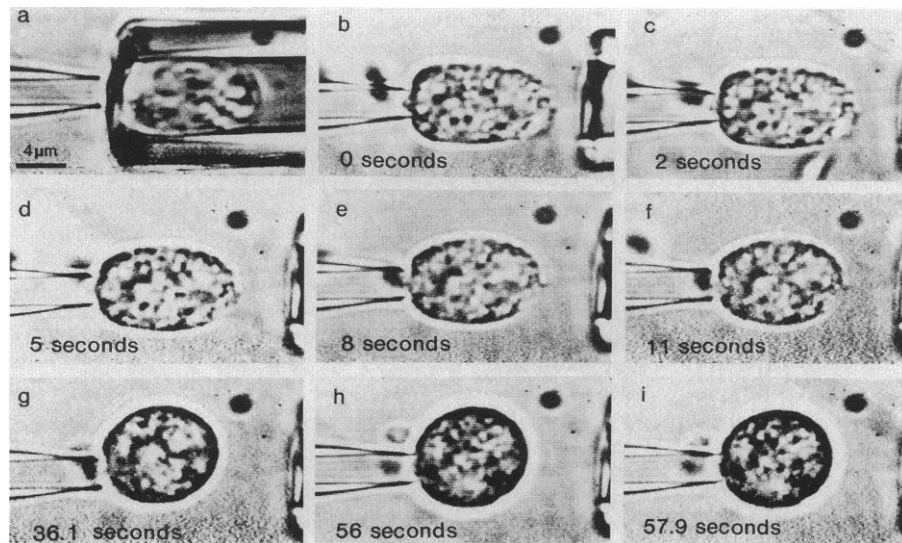


FIGURE 2 (a) Model of the standard viscoelastic solid assumed for leukocyte. (b) Schematic of a leukocyte in recovery associated with cartesian coordinates ( $x, y$ ) and the spherical coordinates ( $r, \phi$ ) in axisymmetrical case (with respect to the central axis  $x$ ).  $a_0$  is the origi cell radius.

FIGURE 1 Time sequence depicting cell recovery upon release from a micropipette. (a) shows the cell inside the pipette. Shows the cell outside the pipette right after release. This corresponds to time  $t = 0$ . The cell is axisymmetrically deformed with respect to the central axis of the micropipette and recovers to a sphere (c–i). A small pipette on the left serves to hold the cell in focus with small aspiration pressure.

where  $\delta_{ij}$  is the Kronecker symbol and  $p$  is the hydrostatic pressure. Let  $u_i$  be the displacement components which are considered as functions of the spatial coordinates and time. The constitutive equation for the standard solid model can be given by (Schmid-Schönbein et al., 1981).

$$\tau_{ij} + \frac{\mu}{k_2} \dot{\tau}_{ij} = k_1 \gamma_{ij} + \mu \left( 1 + \frac{k_1}{k_2} \right) \dot{\gamma}_{ij}. \quad (2)$$

For small deformation, the strain components  $\gamma_{ij}$  can be expressed in the terms of the strain-displacement relations

$$\gamma_{ij} = \frac{1}{2} (u_{i,j} + u_{j,i}). \quad (3)$$

The dots on  $\dot{\tau}_{ij}$  and  $\dot{\gamma}_{ij}$  indicate the time derivatives of stress and strain components, and a comma in  $u_{i,j}$  denotes the derivative of displacement with respect to the spatial coordinates. In Eq. 2,  $k_1$  and  $k_2$  represent two elastic coefficients measured in dyn/cm<sup>2</sup>, and  $\mu$  is a viscous coefficient measured in dyn · s/cm<sup>2</sup> as in Fig. 2 a.

If we neglect all gravitational and inertial forces, the equation of equilibrium for the cell can be then reduced to the form:

$$\sigma_{ij,j} = 0. \quad (4)$$

Using Eqs. 1–3 and the continuity equation for the incompressible material

$$u_{i,i} = 0 \quad (5)$$

Eq. 4 can be written in a vector notation as

$$\frac{1}{J(t)} \nabla^2 \mathbf{u} = \nabla p, \quad (6)$$

where  $J(t)$  is a creep function for the standard viscoelastic solid material derived from Eq. 2 as

$$J(t) = \frac{k_2}{k_1(k_1 + k_2)} \exp \left[ -\frac{k_1 k_2}{\mu(k_1 + k_2)} t \right]. \quad (7)$$

The form of Eqs. 6–7 applies to the solution under release of a step loading which was applied before  $t = 0$ .

The solution of Eq. 6 can be obtained in the spherical coordinate system for the axisymmetric case ( $r, \phi$  in Fig. 2 b) starting from the general solution for an elastic sphere given by Lamb (1945), which is

$$\mathbf{u} = J(t) \sum_{n=1}^{\infty} \left\{ \frac{(n+3)r^2}{2(n+1)(2n+3)} \nabla P_n + \nabla \Phi_n - \frac{n\mathbf{r}}{(n+1)(2n+3)} P_n \right\}, \quad (8)$$

where  $\mathbf{r}$  is the radial position vector and  $P_n, \Phi_n$  are defined as the spherical solid harmonics of order  $n$ .

We assume that the shape of the cell is given at the time it starts the recovery right after expulsion from the micropipette into a free suspension. This gives the initial conditions which lead to the following specific solution from Eq.

8 for the surface response of the leukocyte in cartesian coordinate system ( $x, y$  in Fig. 2 b) with the free stress boundary during recovery as

$$u_x(t) = a_0 J(t) \cdot \sum_{n=1}^{\infty} \left\{ \frac{-\alpha_n n}{2n^2 + 4n + 3} \left[ \frac{3}{2(n-1)} L_{n-1}(\eta) + n L_n(\eta) \right] \right\}$$

$$u_y(t) = a_0 J(t) \cdot \sum_{n=1}^{\infty} \left\{ \frac{\alpha_n (1 - \eta^2)^{1/2}}{2n^2 + 4n + 3} \left[ \frac{3}{2(n-1)} L'_{n-1}(\eta) - n L_n(\eta) \right] \right\} \quad (9)$$

where

- $a_0$  = original cell radius;
- $L_n(\eta)$  = Legendre polynomials of order  $n$ ;
- $L'_n(\eta)$  = the first derivative of  $L_n(\eta)$  with respect to  $\eta$ ;
- $\eta = \cos \phi$ ;
- $\alpha_n$  = coefficients dependent on the dimensions of the cell as initially held inside the micropipette before expulsion.

## RESULTS

All experiments were carried out on neutrophilic leukocytes. When the cells were released from the pipette, an instantaneous recovery was observed (Fig. 1, a and b). The degree of deformation is accurately measured from the major diameter before  $d_1(0^-)$  and after  $d_1(0^+)$  release (this corresponds to time 0). Measurement of the minor diameter before release is uncertain because of light diffraction of the glass wall of the pipette. Due to the geometry of leukocyte whose shape is almost spherical in the resting (undeformed) state (Chien et al., 1984), the cell will be axisymmetrically deformed if the pressure load is applied axisymmetrically with respect to the central axis of the micropipette. Leukocyte can also recover to an approximate sphere when it is released to a free medium after deformation. The initial stretch ratio  $d_1(0^+)/d_1(0^-)$  is shown in Fig. 3 and is of the order or 0.93 for holding times

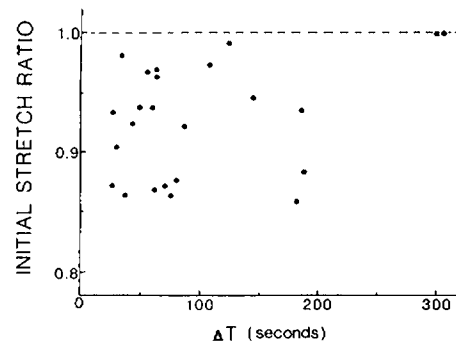


FIGURE 3 Initial stretch ratio  $d_1(0^+)/d_2(0^-)$  of the major cell diameter before ( $d_1(0^-)$ ) and after ( $d_1(0^+)$ ) release from the pipette.  $\Delta T$  is the time period for which the cell is held in the micropipette. Note that except for long periods of time, the cells show a distinct initial elastic recovery.

$\Delta T < 200$  s. For longer holding times, the initial recovery is smaller.

After the initial recoil, a slow exponential recovery was observed in all leukocytes. The major diameter  $d_1$  and minor diameter  $d_2$  as a function of time have been presented (Figs. 4 and 5). This slow recovery was observed for all pipette sizes. The individual experiments were reproducible when the same cell and the same micropipette were used (Fig. 4). The rate of recovery was dependent on the time  $\Delta T$  that the cell was kept inside the pipette. Fig. 6 shows the time to 90% recovery, i.e., such that  $(d_1[t] - d_0)/d_0 = 0.9$ , as a function of  $\Delta T$  for neutrophilic leukocytes. It is apparent that the longer the cell is kept deformed, the slower will be its recovery.

The recovery history is strongly influenced by protopod formation. Fig. 7 shows a specific case where the protopod started to grow at the instant the cell was released. It leads to a more rapid recovery of the main cell body since cytoplasmic material is flowing into the protopod. The exact recovery history varies from case to case of protopod formation depending on the time the protopod starts to grow relative to the passive recovery, the number of protopods present, and whether a protopod pre-existed inside the micropipette during the holding period.

## DISCUSSION

From the previous work (Schmid-Schönbein et al., 1981), a method of determining the model parameters ( $k_1$ ,  $k_2$ , and  $\mu$ ) in a standard viscoelastic solid (Fig. 2a) has been introduced. Fig. 8 shows a comparison of experimental data and theoretical predictions of cell deformation during aspiration (according to Schmid-Schönbein et al., 1981) using the method of least square error to determine the viscoelastic coefficients  $k_1$ ,  $k_2$ , and  $\mu$ . Although this procedure leads to a good prediction of the aspiration for 1 or 2 s,

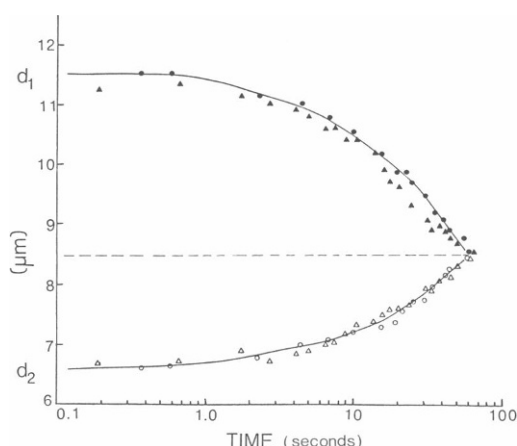


FIGURE 4 Time course of the cell recovery after the initial elastic recoil of a neutrophilic leukocyte. Time is plotted on a logarithmic scale. The round and triangular points represent two recovery histories of the same cell and same micropipette (diameter  $\sim 5.6$   $\mu\text{m}$ ) for the same holding period  $\Delta T = 45$  s. The undeformed cell diameter  $d_0$  is  $\sim 8.5$   $\mu\text{m}$  (dashed line).

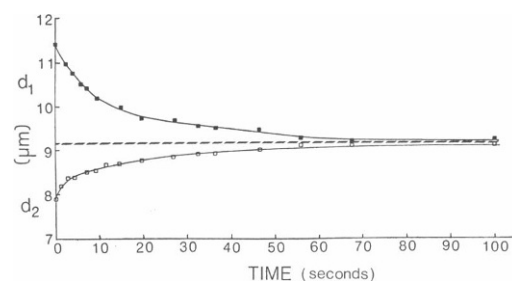


FIGURE 5 Viscoelastic recovery of eosinophilic leukocytes in free suspension after rejection from a micropipette. The curves show the major diameter  $d_1$  and the minor diameter  $d_2$  as a function of time. The pipette diameter  $\sim 7.4$   $\mu\text{m}$ . The cell holding time is  $\Delta T = 60$  s.

it gives a set of parameters (listed in the legend of Fig. 8) which if applied to the relaxation solution in Eq. 9 they give a recovery history faster than the experimental results (Fig. 9). One of the main purposes of the present paper is to show how this discrepancy can be removed. If a different set of empirical coefficients is applied by trial and error selection with high viscosity  $\mu$ , and the lower parallel stiffness  $k_1$ , then the fit to the initial deformation is still satisfactory (Fig. 10) but now the relaxation history can be fitted within experimental error as well (Fig. 11). For smooth initial shapes, the coefficients  $\alpha_n$  in Eq. 9 decrease rapidly with increasing  $n$ . Through the observed leukocyte shapes during recovery experiment, it is found that four terms in  $\alpha_n$  ( $n = 2, 4, 6, 8$ ) are sufficient to approximate the experimental shape closely. The results obtained from the theoretical modeling then show good agreement with the experimental observations on the leukocytes in the micropipette tests.

EDTA is known to both inhibit the spontaneous activation of passive granulocytes and increase the threshold pressure necessary for the onset of deformation of cells into micropipettes (Frank, 1987). In the absence of protopod formation with EDTA, all leukocytes tested in these experiments (neutrophils, eosinophils, and monocytes) exhibited an asymptotic recovery to the undeformed spherical state ( $d_1 = d_2$  in Figs. 4 and 5), which is now reproduced by the standard viscoelastic solid model as

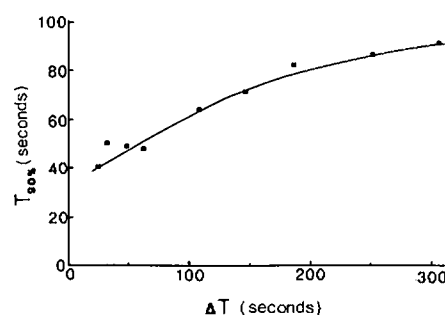


FIGURE 6 The time to 90% cell recovery as a function of the holding period  $\Delta T$ . The pipette diameter is  $\sim 5.6$   $\mu\text{m}$ . The undeformed cell diameter is  $8.5$ – $8.8$   $\mu\text{m}$ .

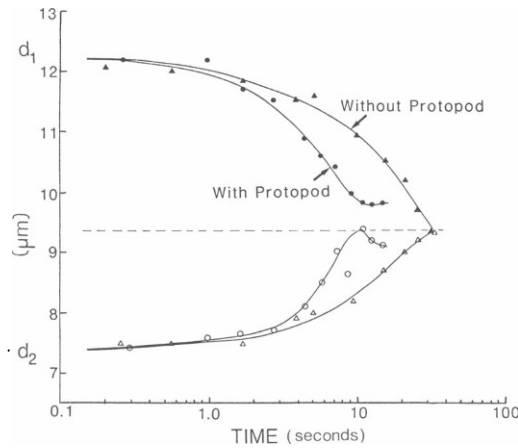


FIGURE 7 The history of cell recovery with and without protopod formation. The cell starts to form a protopod in the direction of the minor axis at the time of release. Since cytoplasmic material streams into the protopod, a much more rapid recovery history of the main cell body is observed. Pipette diameter is  $7.1 \mu\text{m}$  and cell holding period  $\Delta T = 70 \text{ s}$  in both cases.

shown in Fig. 11. This observation also agrees with the recovery history of passive leukocytes for the case of small diameter pipette experiments (Schmid-Schönbein et al., 1981) in which the strains are small and only part of the cell is deformed.

The creep of the main cell body is dramatically affected by protopod formation. Protopods grow by active actin polymerization locally on the surface of the cell and are much stiffer than the main cell body. It is also found that the protopods are more elastic and this adds an additional resistance to creep recovery. Evans (1984) has reported a single creep history which showed an almost linear trend.

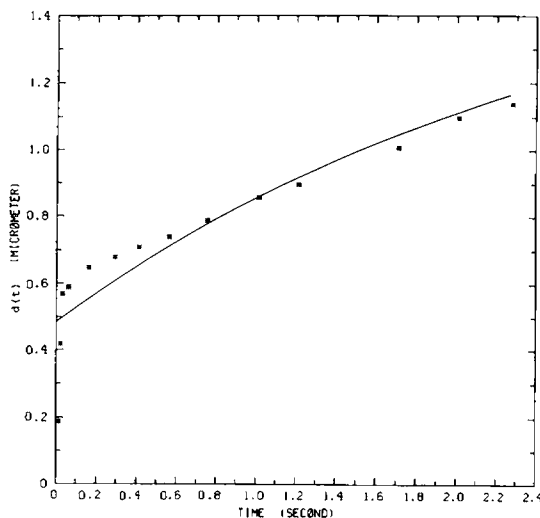


FIGURE 8 Comparison of theoretical displacement  $d(t)$  at cell tongue in the aspiration phase (Schmid-Schönbein et al., 1981) to experimental data (dots). The curve shown corresponds to the model parameters obtained from the least square error method:  $k_1 = 121.2 \text{ dyn/cm}^2$ ,  $k_2 = 293.0 \text{ dyn/cm}^2$ ,  $\mu = 223.8 \text{ dyn} \cdot \text{s/cm}^2$  and the resting cell diameter  $d_0 = 8.05 \mu\text{m}$ .

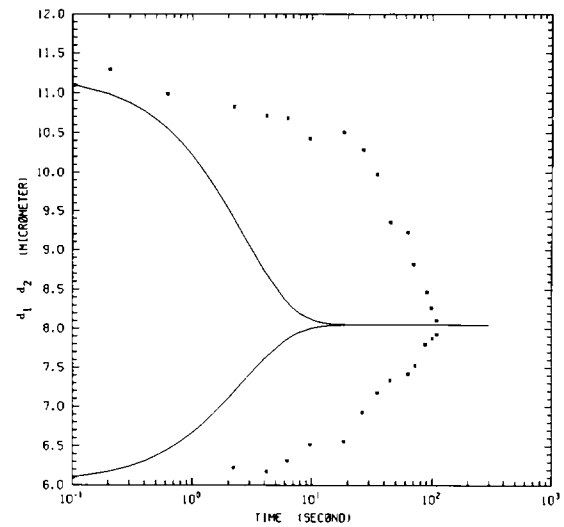


FIGURE 9 Theoretical prediction of the major diameter  $d_1(t)$  and the minor diameter  $d_2(t)$  of the cell in comparison to experimental data (dots). The curves shown are computed for the recovery phase using the same parameters as those to obtain Fig. 8.

Such a recovery is possible in the presence of protopod formation. The time history for recovery may also be prolonged compared with passive cells if a protopod pre-existed inside the pipette during the holding period  $\Delta T$ . Recovery will only start when the protopod starts to retract since the elastic resistance in the stiffer protopod will be then gradually removed.

An interesting feature is that the recovery is essentially axisymmetric for the passive granulocytes and monocytes. This suggests homogeneity among all cytoplasmic rheological properties, despite the presence of microfilaments,

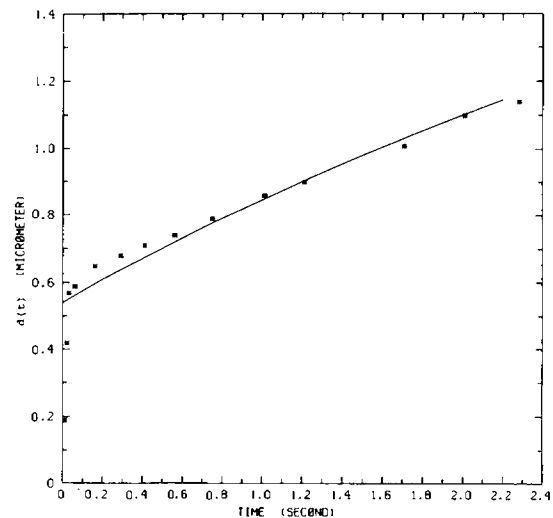


FIGURE 10 Appropriate adjustments of the model parameters ( $k_1$ ,  $k_2$ , and  $\mu$ ) are applied to fit the theoretical displacement  $d(t)$  in the aspiration phase using the solution given by Schmid-Schönbein et al. (1981). The experimental data (dots) is the same as that in Fig. 8 but the theoretical curve is computed by  $k_1 = 7.5 \text{ dyn/cm}^2$ ,  $k_2 = 238.0 \text{ dyn/cm}^2$ ,  $\mu = 330 \text{ dyn} \cdot \text{s/cm}^2$ ; the undeformed cell diameter  $d_0 = 8.05 \mu\text{m}$ .

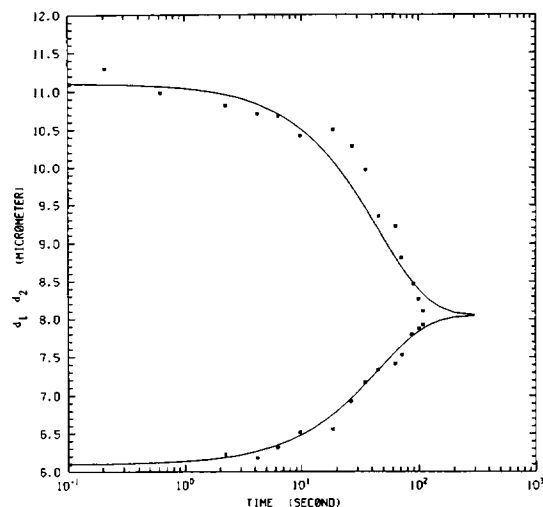


FIGURE 11 Comparison of the diameters  $d_1(t)$  and  $d_2(t)$  to experimental data (same as that used in Fig. 9) in the recovery phase with the adjusted parameters indicated in Fig. 10.

granules, microtubules and the nucleus. This is also in agreement with earlier observations using small diameter pipettes that the deformation history is independent of the location on the surface of the cell. If the cell is aspirated with the same pressure and micropipette, the same deformation is observed at different points on the cell surface within experimental error (Schmid-Schönbein et al., 1981). This isotropy is, however, not expected in active cells or in large deformation with high stresses exerted on the nucleus for prolonged periods of time.

The fact that the deformation history can be fitted with different sets of viscoelastic coefficients ( $k_1$ ,  $k_2$ , and  $\mu$ ) is to a large degree due to the experimental error and the limited time history of the experiments with the small strain assumption of the current theory. However, a set of model coefficients can be selected, that fits both the deformation and recovery behavior of the whole cells. Recovery for smaller strains is more rapid, which suggests that the three coefficients  $k_1$ ,  $k_2$ , and  $\mu$  may not be entirely invariant with respect to strain and strain rate. This feature needs to be explored further with a large strain theory.

Received for publication 3 December 1987 and in final form 22 April 1988.

## REFERENCES

- Bagge, U., R. Skalak, and R. Atefors. 1977. Granulocyte rheology. *Adv. Microcir.* 7:29-48.
- Bagge, U., B. Amundson, and C. Lauritzen. 1980. White blood cell deformability and plugging of skeletal muscle capillaries in hemorrhagic shock. *Acta. Physiol. Scand.* 180:159-163.
- Chien, S., K.-L. P. Sung, G. W. Schmid-Schönbein, A. Tözeren, H. Tözeren, S. Usami, and R. Skalak. 1980. Microrheology of erythrocytes and leukocytes. Symposium on Hemorheology and Diseases. J. F. Stoltz and P. Drouin, editors. Domin Editeurs, Paris. 93-108.
- Chien, S., G. W. Schmid-Schönbein, K.-L. P. Sung, E. A. Schmalzer, and R. Skalak. 1984. Viscoelastic properties of leukocytes. In *White Cell Mechanics: Basic Science and Clinical Aspects*. Alan R. Liss, Inc., New York. 19-51.
- Evans, E. A. 1984. Structural model for passive granulocyte based on mechanical deformation and recovery after deformation test. In *White Cell Mechanics: Basic Science and Clinical Aspects*. Alan R. Liss, Inc., New York. 53-74.
- Frank, R. S. 1987. Alterations in the deformability of passive granulocytes with EDTA. *Adv. Bioeng.* 3:121-122.
- Fung, Y.-C. 1965. *Foundations of Solid Mechanics*. Prentice-Hall, Inc., Englewood Cliffs, New Jersey.
- Lamb, H. 1965. *Hydrodynamics*. 6th ed. Dover Press, London.
- Martz, E. 1975. Early steps in specific tumor cell lysis by sensitized mouse T-lymphocytes: I resolution and characterization. *J. Immunol.* 115:261-267.
- Nathan, C. F., J. A. Mercer-Smith, N. M. Desantis, and M. A. Palladino. 1982. Role of oxygen in T cell-mediated cytotoxicity. *J. Immunol.* 129:2164-2169.
- Nicoll, P. A., and R. L. Webb. 1946. Blood circulation in the subcutaneous tissue of the living bat wing. *Ann. N. Y. Acad. Sci.* 46:697-711.
- Schmid-Schönbein, G. W., K.-L. P. Sung, H. Tözeren, R. Skalak, and S. Chien. 1981. Passive mechanical properties of human leukocytes. *Biophys. J.* 36:243-256.
- Schmid-Schönbein, G. W. 1987. Capillary plugging by granulocytes and the no-reflow phenomenon in the microcirculation. *Fed. Proc.* 46:2397-2401.
- Sung, K.-L. P., G. W. Schmid-Schönbein, R. Skalak, G. B. Schuessler, S. Usami, and S. Chien. 1982. Influence of physicochemical factors on rheology of human neutrophils. *Biophys. J.* 39:101-106.
- Sung, K.-L. P., L. A. Sung, M. Crimmins, S. J. Burakoff, and S. Chien. 1986. Determination of junction avidity of cytotoxic T cell and target cell. *Science (Wash., DC)*. 234:1405-1408.